MNRAS, accepted

GeV emission from Gamma-Ray Burst afterglows

A. Panaitescu
Space Science and Applications, MS D466, Los Alamos National Laboratory, Los Alamos, NM 87545, USA

arXiv:0712.1536v2 [astro-ph] 10 Jan 2008

ABSTRACT

We calculate the GeV afterglow emission expected from a few mechanisms related to GRBs and their afterglows. Given the brightness of the early X-ray afterglow emission measured by Swift/XRT, GLAST/LAT should detect the self-Compton emission from the forward-shock driven by the GRB ejecta into the circumburst medium. Novel features discovered by Swift in X-ray afterglows (plateaus and chromatic light-curve breaks) indicate the existence of a pair-enriched, relativistic outflow located behind the forward shock. Bulk and inverse-Compton upscattering of the prompt GRB emission by such outflows provide another source of GeV afterglow emission detectable by LAT. The large-angle burst emission and synchrotron forward-shock emission are, most likely, too dim at high photon energy to be observed by LAT. The spectral slope of the high-energy afterglow emission and its decay rate (if it can be measured) allow the identification of the mechanism producing the GeV transient emission following GRBs.

Key words: radiation mechanisms: non-thermal - shock waves - gamma-rays: bursts

1 SOURCES OF GEV AFTERGLOW EMISSION

In Gamma-Ray Bursts (GRBs), there are two main sources of GeV afterglow photons. One is the *prompt emission* itself, which lasts for $t_\gamma = 3 - 300$ s (e.g. Sakamoto et al 2007, Willingale et al 2007), has a broken power-law spectrum F_ν peaking at $\epsilon_p \sim 100$ keV, above which $F_\nu \propto \nu^{-\beta_\gamma}$ with $\beta_\gamma \in (0.6, 2.3)$ and a 25 keV – 1 MeV fluence $\phi = 10^{-5\pm1}$ erg cm^{-2} (for long bursts) (e.g. Preece et al 2000). The other one is the *afterglow emission* which, at X-rays, exhibits a plateau at 0.3–30 ks characterized by a 1 keV flux $(\nu F_\nu)_{1keV}(t = 1\text{ks}) = 10^{-11\pm1}$ erg cm^{-2} s^{-1}, a power-law spectrum $F_\nu \propto \nu^{-\beta_x}$ with $\beta_x \in (0.5, 2)$ (e.g. O'Brien et al 2006, Willingale et al 2007) and a power-law decay $F_\nu \propto t^{-\alpha_x}$ with $\alpha_x \in (0, 1)$ (e.g. Nousek et al 2006).

In addition to the above "direct" sources of high-energy (GeV) afterglow photons, a fraction of the hard X-ray photons from burst and soft X-ray photons from afterglow can be upscattered in the GeV range either through inverse-Compton off relativistic electrons or bulk-scattering off a faster part of the outflow. In this work, we evaluate the GeV afterglow fluxes expected from these direct and scattering mechanisms and compare them to the sensitivity of the Large Area Telescope (LAT) at 1 GeV for a 1 ks observation, $(\epsilon F_\epsilon)_{LAT} = 10^{-9}$ erg cm^{-2} s^{-1}, corresponding to 5 photons being collected.

Another mechanism directly related to those at work in GRBs and their afterglows, which can produce *afterglow* emission above 100 MeV is the inverse-Compton scattering of flaring internal-shock emission passing through the forward-shock (Fan & Piran 2006; Wang, Li & Mészáros 2006; Fan et al 2007, Galli & Piro 2007). That scenario is not considered here. Other processes which rely on mechanisms that are not directly related to the production of the GRB and afterglow emissions (e.g. synchrotron emission from VHE protons, synchrotron radiation from pairs and muons produced in photo-hadronic processes) and whose high-energy emission is highly uncertain, are also ignored.

1.1 Large-angle GRB emission

Owing to relativistic beaming and geometrical curvature of spherical GRB source, during the burst, the observer receives emission mainly from a patch moving toward the observer and extending an angle opening $\theta_{grb} = \Gamma_{grb}^{-1}$ as seen from the center of fireball, where Γ_{grb} is the Lorentz factor of the source. Although the burst emission mechanism ceases to operate after 10–100 s, the observer continues to receive emission from regions of the GRB source moving at angles $\theta > \theta_{grb}$ relative to the center–observer axis (Kumar & Panaitescu 2000). This "large-angle" emission arrives at observer at time $t(\theta) = t_\gamma(\theta/\theta_{grb})^2$ and is relativistically boosted by a factor $\mathcal{D}(\theta) = 2\Gamma_{grb}/(1 + \Gamma_{grb}^2\theta^2)$, hence $\mathcal{D}(t) \simeq 2\Gamma_{grb}(t_\gamma/t)$ is progressively decreasing with observer time. From here, it can be shown that the large-angle burst emission at photon energy ϵ above the burst spectral peak energy ϵ_p is $F_\epsilon(t) = F_\epsilon^{(grb)}(t/t_\gamma)^{-2-\beta_\gamma}$, where $F_\epsilon^{(grb)} = F_p(\epsilon/\epsilon_p)^{-\beta_\gamma}$ is the flux at energy ϵ during the burst and F_p is the burst average flux at the photon energy ϵ_p, which can be approximated by $F_p \simeq \Phi/(\epsilon_p t_\gamma)$. Assuming that the power-law spectrum of the prompt emission extends up to above GeV photon energies, the large-angle burst emission at $\epsilon > \epsilon_p$ is given by

$$(\epsilon F_\epsilon)^{(lae)} = \frac{\phi}{t_\gamma}\left(\frac{\epsilon}{\epsilon_p}\right)^{1-\beta_\gamma}\left(\frac{t}{t_\gamma}\right)^{-2-\beta_\gamma} . \quad (1)$$

For the representative burst quantities given in §1, the large-angle flux at photon energy $\epsilon = 1\,\epsilon_9$ GeV is

$$(\epsilon F_\epsilon)^{(lae)} = 10^{-6(\beta_\gamma+1)}\phi_{-5}\,t_{\gamma,1}^{\beta_\gamma+1}\left(\frac{\epsilon_9}{\epsilon_{p,5}}\right)^{\beta_\gamma-1}\left(\frac{t}{1\mathrm{ks}}\right)^{-2-\beta_\gamma}\frac{\mathrm{erg}}{\mathrm{cm^2 s}} \quad (2)$$

where the notation $x_n = x/(10^n$ cgs) was used, the photon energy being measured in eV.

Equation (2) shows that, at 1 ks after trigger, the GeV large-angle emission may be detected by LAT at 1 GeV for (*i*) the hardest bursts ($\beta_\gamma = 0.5$), for which $(\epsilon F_\epsilon)_{1GeV} = 10^{-9}\phi_{-5}t_{\gamma,1}^{1.5}\,\mathrm{erg\,cm^{-2}\,s^{-1}}$, or for (*ii*) the harder ($\beta_\gamma = 1$), longest, and brightest bursts (t_γ>100 s, ϕ>$10^{-4}\mathrm{erg\,cm^{-2}}$), for which $(\epsilon F_\epsilon)_{1GeV} = 10^{-9}\phi_{-4}t_{\gamma,2}^{2}\,\mathrm{erg\,cm^{-2}\,s^{-1}}$. Bursts in either category are extremely rare (perhaps less than 1 percent of BATSE GRBs have those properties), thus is seems very unlikely that the large-angle burst emission could produce 1 GeV photons that LAT can detect at 1 ks from trigger. Owing to its very fast decay, there is a much better chance to detect the large-angle emission at earlier times (e.g. at 100 s).

1.2 Primary afterglow emission

If the soft X-ray (1–10 keV) power-law spectrum measured by the X-Ray Telescope (XRT) on Swift extends over more than 5 orders of magnitude in photon energy above 10 keV, then the observed X-ray flux

$$(\nu F_\nu)_{1keV} = 10^{-11\pm1}(t/1\mathrm{ks})^{-\alpha_x}\ \mathrm{erg\,cm^{-2}\,s^{-1}} \quad (3)$$

implies a GeV afterglow flux $\epsilon F_\epsilon = (\nu F_\nu)_{1keV}(\epsilon/1\,\mathrm{keV})^{1-\beta_x}$ which is

$$(\epsilon F_\epsilon)^{(aglow)} = 10^{-(5+6\beta_x)}(\nu F_\nu)_{1keV,-11}\,\epsilon_9^{1-\beta_x}\ \mathrm{erg\,cm^{-2}\,s^{-1}} . \quad (4)$$

Therefore, LAT-detectable GeV emission arising from the same mechanism as that for the X-ray afterglow emission is obtained for β_x<$(4\pm1)/6$. Such hard spectra are measured for about 10 percent of Swift afterglows.

If the X-ray afterglow is the synchrotron emission from the forward-shock driven by the GRB ejecta into the circumburst medium (Mészáros & Rees 1997), then the assumption that the soft X-ray spectrum $F_\epsilon \propto \nu^{-\beta_x}$ extends up to GeV energies is quite likely wrong, particularly for the harder afterglow spectra (β_x<2/3):

(1) If the soft X-ray band were above the "cooling" frequency (ν_c) of the synchrotron spectrum, then the electrons accelerated by the forward-shock would have a power-law distribution with energy ($\gamma_e m_e c^2$) flatter than $dn_e/d\gamma_e \propto \gamma_e^{-4/3}$, which implies that $dn_e/d\gamma_e$ must have a cut-off at some electron energy for which the synchrotron characteristic frequency is above X-ray. However, that the electrons radiating at 1 GeV must have an energy larger by a factor 10^3 than those radiating at 1 keV, suggests that the synchrotron frequency cut-off associated with the maximum electron energy is below 1 GeV.

(2) If the soft X-ray range is below ν_c, then the GeV flux depends on the exact location of ν_c. For 10 GRB afterglows with a good coverage at radio, optical, and X-ray, through modelling their multiwavelength measurements, we have found shock microphysical parameters, shock kinetic energies, and ambient medium densities for which ν_c should be between optical and soft X-ray at 1 ks (Panaitescu 2005). This suggests that, if other afterglows have similar forward-shock parameters, their cooling frequency is never too much above the soft X-ray range. Taking into account that the spectrum of the forward-shock synchrotron emission should be $F_\epsilon \propto \nu^{-\beta_x-1/2}$ above ν_c, it follows that, for ν_c around 100 keV, the GeV flux is a factor $\sim$ 100 lower than that given in equation (4). Then, the GeV flux from the forward-shock synchrotron emission would be detected by LAT only for the hardest ($\beta_x = 0.5$) and brightest ($(\nu F_\nu)_{1keV} = 10^{-10}\,\mathrm{erg\,cm^{-2}\,s^{-1}}$) afterglows observed by XRT.

If the X-ray afterglow is the forward-shock synchrotron emission upscattered in a different part of the outflow (see §1.4), then the upscattered ν_c could be above 1 MeV and the likelihood of detecting GeV photons from the same mechanism as that yielding the X-ray afterglow will be larger, although still restricted to a minority of afterglows with the hardest X-ray emission.

1.3 Self-Compton scattering of afterglow emission

We consider now the upscattering of the X-ray synchrotron forward-shock emission by the same electrons, the model for GeV *afterglow* emission that has received most attention so far (e.g. Mészáros & Rees 1994, Panaitescu & Mészáros 1997, Dermer, Chiang & Mitman 2000, Zhang & Mészáros 2001, Pe'er & Waxman 2005, Fan et al 2007). Galli & Piro (2007) offer a detailed treatment of this emission and comparison with LAT's detection capability. In contrast to these works, we want to estimate the GeV inverse-Compton flux expected for the observed X-ray synchrotron forward-shock flux by making minimal use of the usual afterglow parameters.

At a photon energy above the peak frequency of the scattered emission ($\epsilon_p^{(ic)}$), the flux of the inverse-Compton forward-shock emission is

$$(\epsilon F_\epsilon)^{(ic)} = (\epsilon F_\epsilon)_p^{(ic)}(\epsilon/\epsilon_p^{(ic)})^{1-\beta_x} \quad (5)$$

where $F_{\epsilon,p}^{(ic)}$ is the peak flux of the inverse-Compton afterglow spectrum. The spectral quantities of the upscattered emission can be related to those of the synchrotron's:

$$\epsilon_p^{(ic)} = \gamma_e^2\epsilon_p^{(sy)} , \quad F_{\epsilon,p}^{(ic)} = \tau_e F_{\epsilon,p}^{(sy)} \quad (6)$$

where γ_e is the Lorentz factor of the electrons which radiate at the peak frequency $\epsilon_p^{(sy)}$ and τ_e is the optical thickness of the forward-shock to electron scattering. The observed X-ray emission at 1 keV is $(\nu F_\nu)_{1keV} = (\epsilon F_\epsilon)_p^{(sy)}(1\,\mathrm{keV}/\epsilon_p^{(sy)})^{1-\beta_x}$, thus

$$(\epsilon F_\epsilon)^{(ic)} = (\nu F_\nu)_{1keV}\,(\epsilon/1\,\mathrm{keV})^{1-\beta_x}\gamma_e^{2\beta_x}\tau_e . \quad (7)$$

If the GRB progenitor is a Wolf-Rayet star, the mass swept-up by the forward-shock is $M_{fs} = (dM/dt)R/v = 6\times10^{28}R_{16}$ g, assuming a typical mass-loss rate $dM/dt = 10^{-5}M_\odot\mathrm{yr}^{-1}$ and wind velocity $v = 10^3\,\mathrm{km\,s^{-1}}$). Conservation of the forward-shock energy E_{fs} during its interaction with the stellar wind, $E_{fs} = \Gamma_{fs}^2 M_{fs}c^2$, and the relation between the shocks radius and the arrival time of photons emitted by the region moving at an angle Γ_{fs}^{-1} relative to the direction toward the observer, $R_{fs} \simeq \Gamma_{fs}^2 ct$, lead to a Lorentz factor of the shocked circumburst medium

$$\Gamma_{fs} = 42\,(E_{fs,53}/A_*)^{1/4}\,(t/1\mathrm{ks})^{-1/4} \quad (8)$$

and radius

$$R_{fs} = 2.3\times10^{16}(E_{fs,53}/A_*)^{1/2}\,(t/1\mathrm{ks})^{1/2}\,\mathrm{cm} \quad (9)$$

for a burst at redshift $z = 2$, where $A_* \equiv (dM/dt)/(10^{-5}M_\odot\mathrm{yr}^{-1})\times(10^3\,\mathrm{km\,s^{-1}}/v)$ (for Galactic WR stars, the wind parameter A_* varies from 0.3 to 2 – Nugis & Lamers 2000). Therefore, the forward-shock optical thickness to electron scattering is

$$\tau_e = \frac{\sigma_e M_{fs}}{4\pi m_p R_{fs}^2} \simeq 10^{-5}E_{fs,53}^{-1/2}A_*^{3/2}\,(t/1\mathrm{ks})^{-1/2} \quad (10)$$

where σ_e is the Thomson cross-section for electron scattering.

The hardest X-ray spectra ($\beta_x \simeq 1/2$) measured by XRT indicate that, at least for some afterglow, the cooling frequency of the synchrotron emission is above X-ray. For simplicity, we assume that this generally valid, hence γ_e of equation (7)) is the typical Lorentz factor of the electrons accelerated by the forward-shock, parameterized by the fraction of the post-shock energy that the electrons acquire (if they all had same Lorentz factor γ_e) :

$$\gamma_e\,m_ec^2 = \varepsilon_e\,\Gamma_{fs}\,m_pc^2 \quad (11)$$

where $\Gamma_{fs}m_pc^2$ is its internal energy per proton. Then, equation (8) leads to

$$\gamma_e = 3800\;(\varepsilon_e/0.05)(E_{fs,53}/A_*)^{1/4}\,(t/1\mathrm{ks})^{-1/4} \quad (12)$$

where the fractional electron energy was normalized to the maximum value found by Panaitescu (2005) from modelling the afterglow emission. XRT observations show that the peak frequency of the synchrotron forward-shock spectrum ($\epsilon_p^{(sy)}$) is below 0.3 keV before 1 ks after trigger thus, for the electron Lorentz factor of equation (12), the peak frequency of the upscattered emission ($\epsilon_p^{(ic)}$) at 1 ks should be below the GeV range.

Combining equations (7), (10), and (12), we obtain that, for the X-ray flux typically measured by XRT (equation 3), the flux of the forward-shock self-Compton flux should be

$$(\epsilon F_\epsilon)^{(ic)} \le 10^{-10+1.2\beta_x}\left(\frac{\varepsilon_e}{0.05}\right)^{2\beta_x}E_{fs,53}^{\frac{\beta_x-1}{2}}A_*^{\frac{3-\beta_x}{2}}$$
$$\times(\nu F_\nu)_{1keV,-11}\epsilon_9^{1-\beta_x}\left(\frac{t}{1\mathrm{ks}}\right)^{-\frac{\beta_x+1}{2}}\frac{\mathrm{erg}}{\mathrm{cm^2s}} \quad (13)$$

with a weak dependence on the forward-shock's kinetic energy. Therefore, for the typical $\beta_x = 1$ measured by XRT, X-ray afterglows brighter than average should be accompanied by inverse-Compton emission detectable to LAT.

1.4 Bulk-scattering of GRB emission

Most of the X-ray afterglows monitored by Swift exhibit *flares* and light-curve *plateaus* at 0.1–10 ks after trigger. Most flares evolve on a timescale shorter than the time when they occur (Burrows et al 2007, Chincarini et al 2007), which indicates that they are not from the forward-shock. Instead, flares have been attributed (e.g. Zhang et al 2006) to the same mechanism (perhaps synchrotron and/or self-Compton emission from *internal shocks* in a relativistic, unstable outflow – Rees & Mészáros 1994) that produces the highly-variable burst emission. Therefore, this scenario for X-ray flares require a long-lived central engine, expelling relativistic outflows at lab-frame times comparable to the observer time when the flares are seen.

During the X-ray plateau, the 0.3–10 keV afterglow flux decays slower than expected for the forward-shock synchrotron emission, which prompted speculations that (at least one) of the basic assumptions is invalid. One plausible scenario is that energy is injected into the forward-shock by means of some late ejecta which catch-up with the forward shock as the latter undergoes deceleration by sweeping-up the ambient medium (Nousek et al 2006, Panaitescu et al 2006a, Zhang et al 2006). In that case, the plateau end marks a change in (e.g. cessation of) the power injected in the forward-shock. However, this interpretation encounters the following problem: a change in the forward-shock dynamics should be manifested in the afterglow light-curve at all frequencies, yet about half of the plateau ends which have been monitored in the optical do not occur in the optical as well, i.e. are *chromatic* (Watson et al 2006, Panaitescu et al 2006b). An alternative explanation for such chromatic X-ray light-curve breaks – the passage of a spectral break through the X-ray – is ruled out by that the hardness of the X-ray continuum does not evolve across the light-curve break (Willingale et al 2007, Liang et al 2007).

Thus, the existence of X-ray flares and plateaus suggest a sustained ejection of relativistic material, but the chromatic X-ray breaks cannot be explained by the injection of energy into the forward-shock produced by the late outflow catching-up with the shock. Instead, those chromatic X-ray breaks suggest that there is a contribution to the afterglow flux that does not arise from the forward shock.

As shown by Panaitescu (2007), bulk scattering of the forward-shock emission off the extended outflow required by X-ray flares can account for the observed decoupling of the optical and X-ray emissions because the scattered emission is likely to overshine that coming directly from the forward-shock only at higher (X-ray) but not at lower (optical) photon energies. For this to happen, the scattering outflow, inner to the forward-shock, must (1) move at a higher Lorentz factor (which is a natural consequence of the forward-shock deceleration caused by its interaction with the circumburst medium) and, quite likely, (2) should be enriched with leptons above what is expected for normal, baryonic ejecta (which suggests that the scattering outflow is not accelerated from within the collapsing star but, instead, it results from the dissipation of magnetic fields at large distances from the progenitor – the electromagnetic model of Lyutikov 2006a). The first condition above implies that the brightness of the scattered emission received by observer at time t depends on the Lorentz factor and mass-flux (i.e. optical thickness) in the scattering outflow at a distance ct behind the forward-shock, consequently the observer-frame duration of the X-ray light-curve plateau is equal to the lab-frame light travel-time between the inner edge of the scattering outflow and the GRB source.

In addition to X-ray plateaus and chromatic breaks, the scattering model can also explain the short duration of X-ray flares (Shen et al 2007 have investigated the brightness of X-ray flares resulting from scattering the burst emission off geometrically thin, relativistic outflows) and the observed diversity of post-plateau decays, some of which display very fast decays (t^{-3} to t^{-9}). The former arises from that the re-

flection of the photons emitted by the forward-shock (moving at Γ_{fs}) off a surface moving at a higher Lorentz factor (Γ_{sc}) reduces observer-frame timescales by a factor $\Gamma_{fs}^2/\Gamma_{sc}^2$. The latter feature is naturally accommodated because the decay of the scattered emission depends on the radial distribution of mass-flux and Lorentz factor in the scattering outflow.

A pair-rich outflow located behind the forward-shock provides two ways to produce GeV afterglow photons. One is the scattering of X-ray forward-shock photons to higher energies. If the X-ray-to-GeV photons arise from this mechanism then the fluxes at low and high photon energies are related through equation (4). As noted in §1.2, in this model, the upscattered cooling frequency could be above 1 MeV, thus the scattered forward-shock emission of the brightest and hardest X-ray afterglows may be detected by LAT.

GeV photons are also produced through scattering of the prompt, GRB emission. The dependence of the scattered GRB emission on the various burst and scattering outflow parameters can be obtained as follows. For seed photons moving radially inward and scattered photons moving radially outward along the observer–center of explosion, the Doppler factor for the scatterer–GRB source relative motion is $\mathcal{D}=\Gamma_{sc}/\Gamma_{grb}$. Taking into account that (*i*) the observed scattered and seed photon energies are a larger by a factor Γ_{sc} and Γ_{grb}, respectively, than in the corresponding source frame, (*ii*) bulk-scattering increases the energy of the seed photon by a factor $\mathcal{D}$, and (*iii*) if the scattering electrons are hot (of random Lorentz factor γ_e), then inverse-Compton scattering boosts the energy of the primary photon by a factor γ_e^2 (in the frame of the scattering outflow), it follows that the peak of the scattered emission is at a photon energy

$$\epsilon_p^{(sc)} = (\Gamma_{sc}\gamma_e/\Gamma_{grb})^2\epsilon_p \tag{14}$$

where ϵ_p is the peak photon energy of the burst spectrum. If the scatterer were infinitesimally thin (a surface), then the spectral peak flux of the scattered emission would be

$$F_p^{(sc)} = (1-e^{-\tau_e})(\Gamma_{sc}/\Gamma_{grb})^2 F_p \tag{15}$$

where F_p is the burst flux at the peak of its spectrum. The first factor represents the fraction of incident photons that are upscattered, the second is the product of a factor Γ_{sc}/Γ_{grb} accounting for the effect of time contraction on the received peak-fluxes and a factor $\mathcal{D}$ accounting for the effect of scattering due to the relative motion of the scatterer and GRB source. We note that the motion of the two sources toward the observer does enhance the comoving specific intensities by factors Γ_{sc}^3 and Γ_{grb}^2 (one factor for time contraction, two powers for angular beaming), however the received fluxes "lose" the angular-beaming factor Γ^2 because this effect also reduces the fractional area of the spherical source whose emission is beamed toward the observer by a factor Γ^2. The relative motion of the scatterer and GRB source enhances the intensity of the incident flux by a factor $\mathcal{D}^3$; however, in the scatterer's frame, the highly collimated incident flux, arriving from within $\mathcal{D}^{-2}$ around the radial direction of motion (owing to relativistic beaming) is nearly isotropically redistributed by electron scattering, hence the net increase in intensity produced by scattering is just a factor $\mathcal{D}$.

The GRB emission scattered by a surface is spread (in the observer frame) over a time $\delta t_{sc} = (\Gamma_{grb}/\Gamma_{sc})^2 t_\gamma$ (this is both the angular spread in the photon arrival time and the time to sweep-up the photons released by the GRB source). For a radially-extended scattering outflow, the scattered GRB emission is further spread over an observer-frame equal to the light travel-time from the inner to the outer edges of the scattering outflow. As the X-ray plateau results from upscattering by the same outflow (but of the forward-shock emission), the geometrical thickness of the scattering outflow is approximately equal to the duration t_X of the X-ray plateau. Therefore, for $\Gamma_{sc} \gtrsim \Gamma_{grb}$, a burst duration $t_\gamma \lesssim 300$ s, and an X-ray plateau lasting for $t_X \sim 10$ ks, the photon arrival-time spread arising from the radial extent of the scattering outflow is dominant and the received flux is lower than that given in equation (15) by a factor $\delta t_{sc}/t_X$.

The scattering outflow lags by $t_X < 10$ ks behind the GRB source, whose radius is $R_\gamma/c = \Gamma_{grb}^2 t_\gamma = 100\,\Gamma_{grb,2}^2 t_{\gamma,1}$ ks ⋆ . Thus, the radius of the scattering outflow can be approximated by that of the GRB source, hence the evolution of the scatterer's optical thickness ($\tau_e \propto R_\gamma^{-2}$) is

$$\tau_e = \frac{t_0^2}{t^2},\ t_0 \equiv \left(\frac{\sigma_e E_{sc}}{4\pi\,\Gamma_{sc}\gamma_e\Gamma_{grb}^4 m_e c^4}\right)^{1/2} = \frac{2.7\,\mathrm{s}}{\Gamma_{grb,2}^2}\left(\frac{E_{sc,53}}{(\Gamma_{sc}\gamma_e)_4}\right)^{1/2} \tag{16}$$

for a pair-dominated outflow of kinetic energy E_{sc}. The product $\Gamma_{sc}\gamma_e$ was scaled to 10^4, for which the scattered spectrum peaks at 1 GeV (equation 14, with $\Gamma_{grb} = 100$ and $\epsilon_p \simeq 100$ keV). By integrating $1-e^{-\tau_e}$ over the evolution given in equation (16), it can be shown that the average fraction of scattered photons is $2t_0/t_\gamma$, for $t_0 < t_\gamma$.

Putting together all these factors, the peak flux of the scattered emission (equation 15) satisfies

$$F_p^{(sc)} \propto \frac{t_0}{t_\gamma}\left(\frac{\Gamma_{sc}}{\Gamma_{grb}}\right)^2 \frac{\delta t_{sc}}{t_X} F_p = \frac{t_0}{t_X} F_p \tag{17}$$

The spectrum of the scattered emission above its peak $\epsilon_p^{(sc)}$ has the same slope as the burst spectrum above ϵ_p, thus $F_\epsilon^{(sc)} \propto F_p^{(sc)}(\epsilon/\epsilon_p^{(sc)})^{-\beta_\gamma}$. Then equations (14) and (17) for the spectral characteristics of the scattered emission spectrum lead to

$$(\epsilon F_\epsilon)^{(sc)} \propto \frac{\phi}{t_\gamma}\frac{E_{sc}^{1/2}}{t_X}\frac{(\Gamma_{sc}\gamma_e)^{2\beta_\gamma-1/2}}{\Gamma_{grb}^{2\beta_\gamma+2}}\left(\frac{\epsilon_p}{\epsilon}\right)^{\beta_\gamma-1} \tag{18}$$

where ϕ is the GRB fluence and $\epsilon_p F_p \simeq \phi/t_\gamma$ was used.

In the derivation of equation (18), we have considered only scattered photons that move along the observer–center direction, for which $\mathcal{D} = \Gamma_{sc}/\Gamma_{grb}$. For incident photons moving along other directions and being scattered toward

⋆ A GRB source radius larger than 10^{15} cm is obtained by Lyutikov (2006b) from the timing of the GRB tail, assuming $\Gamma_{grb} \gtrsim 100$. A similarly large burst radius is obtained by Kumar et al (2007) for a set of 10 GRBs from the the GRB tail epoch and from that the forward-shock is already decelerating when the X-ray afterglow emission emerges. Then, the $10^{-3}-1$ s variability timescale typically observed can be accommodated if the GRB emission arises from hot-spots whose angular extent is (much) smaller than the visible area of opening Γ_{grb}^{-1}. Alternatively, if the burst emission arises from the entire Γ_{grb}^{-1} visible area, the burst variability timescale and the assumed GRB radius require a Γ_{grb} larger by a factor 3–100 than considered here and a correspondingly larger Γ_{sc}.

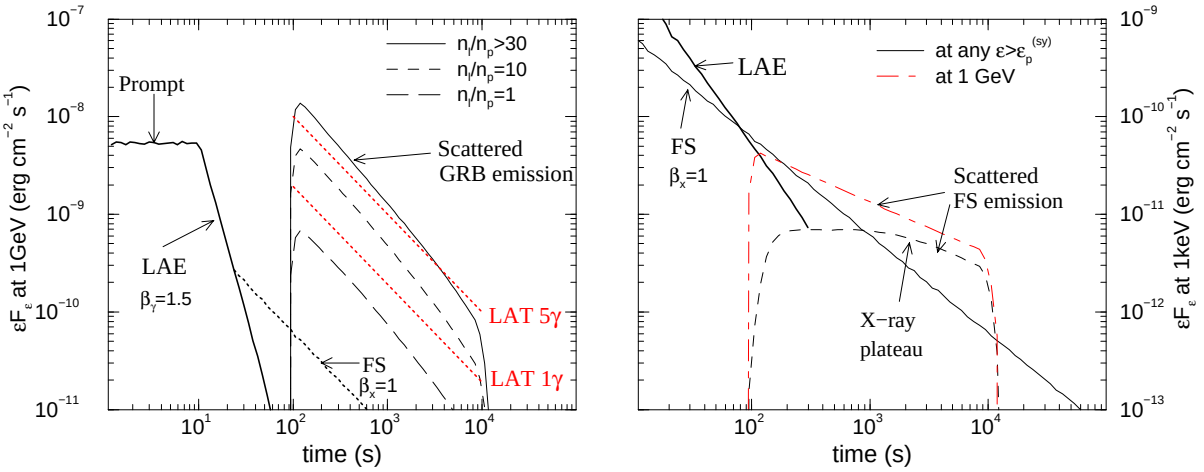


Figure 1. Right panel: X-ray plateau and 1 GeV emission from scattering the *forward-shock* (FS) synchrotron emission by a delayed, lepton-rich ($n_{l(epton)} \gg n_{p(roton)}$), relativistic outflow. Also shown are the X-ray direct FS emissions (for spectral slope $\beta_x = 1$) and the delayed *large-angle emission* (LAE) released during the burst but arriving later at observer. The forward-shock energy is 10^{53} ergs (comparable to the GRB output) and the circumburst medium has the radial density distribution expected for a Wolf-Rayet wind. The scattering outflow properties (see below) were chosen so that the scattered flux overshines that of the forward shock and yields a flux of 10^{-11} erg cm^{-2} s^{-1} at 1 keV with a spectral slope $\beta_x = 1$ (average values measured by XRT). In this case, neither the direct synchrotron FS nor the scattered emission are detectable by LAT. **Left panel**: GeV emission resulting from scattering the ~ 100 keV *burst* emission can be detected by LAT if the scattering outflow is pair-enriched (n_l>10 n_p), as required to produce an X-ray plateau. Red dotted lines labelled "LAT" indicate the 1 GeV flux corresponding to LAT detecting 1 and 5 photons for an integration time equal to the time given on abscissa. The burst spectral peak flux was set to 2 mJy which, for a 10 s burst with a $F_\epsilon \propto \epsilon^{1/3}$ below its 100 keV peak and $F_\epsilon \propto \epsilon^{-1.5}$ above it, corresponds to a 25–1000 keV fluence of 10^{-5} erg cm^{-2} (average parameters for BATSE long bursts). The Lorentz factor of the GRB source (ahead of the scattering outflow) is 100. **Both panels**: The scattering outflow has a kinetic energy of 10^{53} ergs, a scattering parameter $\Gamma\gamma_e = 10^4$ and is radially extended, being initially $10^2 - 10^4$ light-seconds behind the forward shock. This gap introduces a delay between the arrival times of the direct and scattered burst emissions. The radial distribution of scattering outflow's Lorentz factor and mass were assumed to be uniform.

the observer, the relativistic boost associated with the GRB source–scatterer relative motion is much smaller. In the numerical integration of the scattered emission, we take into account that dependence of relativistic beaming of the incoming GRB emission on the angle at which the photon moves (relative to the radial direction), as well as other factors (e.g. the decrease of the scatterer's optical thickness as it expands, the effect of the source's geometrical curvature on the photon arrival time and energy). The numerical calculation of the scattered GRB emission confirms the dependence of the scattered flux on the model parameters given in equation (18), sets its normalization and temporal evolution (Figure 1):

$$(\epsilon F_\epsilon)^{(sc)} = 10^{-9} \frac{\phi_{-5}}{t_{\gamma,1}} \frac{E_{sc,53}^{1/2}}{t_{X,4}} \frac{(\Gamma_{sc}\gamma_e)_4^{2\beta_\gamma - 0.5}}{\Gamma_{grb,2}^{2\beta_\gamma+2}} \left(\frac{\epsilon_9}{\epsilon_{p,5}}\right)^{1-\beta_\gamma} \left(\frac{t}{1\mathrm{ks}}\right)^{-1} \frac{\mathrm{erg}}{\mathrm{cm^2 s}}. \quad (19)$$

The above decay of the scattered emission is obtained for a uniform scattering outflow, in which the ejecta mass dM/dt and Lorentz factor Γ_{sc} are constant. Various decays can be obtained if these quantities vary with the depth ct in the scattering outflow, e.g. for $dM/dt \propto t^m$ and $\Gamma_{sc} \propto t^g$, the scattered flux above $\epsilon_p^{(sc)}$ evolves as $F_\epsilon^{(sc)} \propto t^{m+(2\beta_\gamma-0.5)g-1}$.

Equation (19) indicates that LAT will detect the scattered GRB emission for (1) brighter bursts ($\phi/t_\gamma > 10^{-6}$ erg cm^{-2} s^{-1}) and/or (2) afterglows with shorter plateaus (t_X<10 ks).

2 PAIR-FORMATION OPACITY FOR GEV PHOTONS

For a test photon of energy ϵ emitted at radius R by a source moving at Lorentz factor Γ, most of the optical thickness to pair-formation on photons *from same source* arises as the test photon travels a distance of order R (because of the dilution of photons – $n_\gamma \propto R^{-2}$). The relativistic motion of the source collimates most photons within an angle $\theta = \Gamma^{-1}$ around the radial direction. For this reason, during a small radial displacement dr, the test photon crosses a distance $dr/(2\Gamma^2)$ of the photon front (defined by the location of photons moving at angle Γ^{-1} relative to the test photon), thus the corresponding infinitesimal optical thickness to pair-formation $d\tau_{\gamma\gamma} = (dr/2\Gamma^2)\sigma_{\gamma\gamma} n(\epsilon)$, where $n(\epsilon)$ is the lab-frame density of the target photons with which the test photon can form pairs. Integrating from R to $2R$ over the dilution of target photons and using the upper limit of $\simeq (1/4)\sigma_e$ for the cross-section $\sigma_{\gamma\gamma}$ for pair-formation, we obtain

$$\tau_{\gamma\gamma}(\epsilon) \lesssim \frac{\sigma_e N[>\epsilon_t(\epsilon)]}{32\pi R^2} \quad (20)$$

where $N(>\epsilon_t)$ is the number of photons above the threshold energy ϵ_t for pair-formation on a test photon of energy ϵ, contained in a slab of thickness $R/(2\Gamma^2)$ ahead of the shell at radius R (i.e. the number of photons emitted from observer-frame time $t(R)$ to $2t(R)$).

We estimate now the number $N(>\epsilon_t)$ of target photons emitted by a source of flux $(\epsilon F_\epsilon)_{1GeV} = 10^{-9}(\epsilon F_\epsilon)_{-9}$

erg cm^{-2} s^{-1} (normalization chosen for 5 photons collected by LAT in a 1 ks observation) during $t-2t$, for an observer-frame test photon of energy $\epsilon = 1\,\epsilon_9$ GeV.

For a high-energy flux with the above properties, the number of photons with lab-frame energy above $(z+1)\epsilon$ emitted from observer time t to $2t$ is

$$N[>(z+1)\epsilon]=\frac{4\pi d_l^2(z)\epsilon F_\epsilon}{(z+1)\epsilon}\frac{t}{z+1}=10^{54.3}\left(\frac{z+1}{3}\right)^2\frac{(\epsilon F_\epsilon)_{-9}}{\epsilon_9}\frac{t}{1\rm ks} \quad (21)$$

where $d_l \simeq 5\times10^{27}(z+1)^2$cm is the luminosity distance; this approximation is within 25 percent of the correct value for $z\in(0.5,5)$. The condition for pair-formation $\epsilon_{target}\epsilon_{test}(1-\cos\theta) \geq 2(m_ec^2)^2$ and that most target photons move at angle $\theta \lesssim \Gamma^{-1}$ relative to the test photon, imply that the lab-frame minimum energy ϵ_t of a target photon with which the test photon of observer-frame energy ϵ can form a pair is

$$\epsilon_t(\epsilon) = 350\,[(z+1)/3]^{-1}\Gamma^2\epsilon_9^{-1}\ {\rm eV}\ . \quad (22)$$

For a $F_\epsilon \propto \epsilon^{-\beta}$ spectrum, the number of photons with energy above ϵ_t is

$$N[>\epsilon_t(\epsilon)] = [\epsilon_t/(z+1)\epsilon]^{-\beta}N[>(z+1)\epsilon]$$
$$= 10^{54.3+7\beta}[(z+1)/3]^{2\beta+2}\Gamma^{-2\beta}(\epsilon F_\epsilon)_{-9}(t/1{\rm ks})\,\epsilon_9^{2\beta-1}. \quad (23)$$

To complete the calculation of the optical thickness to pair-formation, the radius and Lorentz factor of the GeV source must be specified. We restrict attention to the two mechanisms which are most likely to yield a LAT-detectable emission at 1 GeV: inverse-Compton scatterings in the forward shock (§1.3) and bulk-scattering of the burst emission in a delayed outflow (§1.4).

2.1 Self-Compton forward-shock emission

For the forward-shock Lorentz factor given in equation (8), the lab-frame threshold energy of the target photon (equation 22) with which a test photon can annihilate is

$$\epsilon_t = 0.6\,[(z+1)/3]^{-1/2}(E_{fs,53}/A_*)^{1/2}(t/1{\rm ks})^{-1/2}\epsilon_9^{-1}\ {\rm MeV} \quad (24)$$

which is around 200 keV in the observer frame. The peak energy of the inverse-Compton spectrum ($\epsilon_p^{(ic)}$) is very likely below 1 GeV but may be above the threshold energy ϵ_t. For $\epsilon_p^{(ic)}>\epsilon_t$, the number of photons above the threshold ϵ_t increases with decreasing spectral peak energy $\epsilon_p^{(ic)}$, thus an upper limit on the optical thickness to pair-formation is obtained by assuming that $\epsilon_p^{(ic)}<\epsilon_t$. Then, the number of target photons is obtained by substituting the forward-shock Lorentz factor of equation (8) in equation (23): $N(>\epsilon_t)< 10^{54.3+3.7\beta_x}[(z+1)/3]^{1.5\beta_x+2}(\epsilon F_\epsilon)_{-9}(A_*/E_{fs,53})^{\frac12\beta_x}$ $(t/1{\rm ks})^{\frac12(\beta_x+1)}\ \epsilon_9^{2\beta_x-1}$. Together with the forward-shock radius given by equation (9), the optical thickness to pair-formation of equation (20) is

$$\tau_{ic,ic} < 10^{3.7\beta_x-4.6}\left(\frac{z+1}{3}\right)^{\frac32\beta_x+3}(\epsilon F_\epsilon)_{-9}\left(\frac{A_*}{E_{fs,53}}\right)^{\frac12\beta_x+1}$$
$$\times(t/1{\rm ks})^{\frac12(\beta_x-1)}\epsilon_9^{2\beta_x-1}. \quad (25)$$

Thus, pair-opacity for the inverse-Compton forward-shock emission at 1 GeV could be important in soft X-ray afterglows ($\beta_x>5/4$) if the peak energy of the upscattered emission spectrum is at only 200 keV. We note that, if the forward-shock microphysical parameters inferred by modelling the broadband emission of 10 afterglows (Panaitescu 2005) are representative, then we expect the peak of the inverse-Compton spectrum to be above 1 MeV at 1 ks. For a tenfold increase of the upscattered peak energy, the optical thickness of equation (25) decreases by a factor 10^{β_x}, thus it seems quite likely that, even for the hardest observed X-ray afterglows ($\beta_x\simeq1.5$), the self-Compton scattering emission is optically thin to pair-formation at 1 GeV.

The test photon may also form pair on a forward-shock synchrotron photon. If the X-ray plateau emission is synchrotron from forward-shock, then the number of these photons can be calculated by using the typical X-ray plateau flux (equation 3) in equation (21). Then, the number of target photons above the threshold energy given in equation (24) is $N_{sy}(>\epsilon_t) = 10^{58.3-2.3\beta_x}[(z+1)/3]^{1.5\beta_x+2}$ $(\nu F_\nu)_{1keV,-11}E_{fs,53}^{-\beta_x/2}(t/1{\rm ks})^{\frac12(1+\beta_x)}\epsilon_9^{\beta_x}$, from where the optical thickness to pair-formation on forward-shock synchrotron photons is

$$\tau_{ic,sy} < 10^{-2.3\beta_x-0.6}\left(\frac{z+1}{3}\right)^{\frac32\beta_x+3}\left(\frac{A_*}{E_{fs,53}}\right)^{\frac12\beta_x+1}$$
$$\times(\nu F_\nu)_{1keV,-11}(t/1{\rm ks})^{\frac12(\beta_x-1)}\epsilon_9^{\beta_x}\ . \quad (26)$$

Equations (25) and (26), with the GeV flux of equation (13), show that pair-formation on forward-shock synchrotron photons could be more important than on inverse-Compton photons for the harder X-ray afterglows with $\beta_x<0.7$, provided that the forward-shock synchrotron spectrum extends above the threshold energy ϵ_t of equation (24) and the self-Compton spectrum peaks below the same ϵ_t.

The Klein-Nishina effect reduces the scattered flux at photon energies approaching the observer frame energy of the scattering electron, i.e. below $\Gamma_{fs}\gamma_e m_ec^2/(z+1)$. Equations (8) and (12) yield a KN cut-off energy $\epsilon_* = 30\,[(z+1)/3]^{-1/2}(\varepsilon_e/0.05)(E_{fs,53}/A_*t_3)^{1/2}$GeV. Because the electrons accelerated at the forward-shock have a power-law distribution with energy above that given in equation (12), the actual cut-off of the inverse-Compton spectrum may be well above ϵ_*.

2.2 Scattered burst emission

For a scattering outflow that is more relativistic than the GRB source ($\Gamma_{sc}\gtrsim100\,\Gamma_{grb,2}$), equation (22) shows that the threshold energy for the target photon is $\epsilon_t = 350\,\Gamma_{sc,3}^2\epsilon_9$ MeV. Substituting the GRB source radius

$$R_{grb} = \Gamma_{grb}^2\frac{ct_\gamma}{z+1} = 10^{15}\ \Gamma_{grb,2}^2\frac{t_{\gamma,1}}{(z+1)/3}\ {\rm cm} \quad (27)$$

in equation (20) and using equation (23) with $\Gamma=\Gamma_{grb}$, the optical thickness to pair-formation for the scattered GRB emission is

$$\tau_{sc,sc} \lesssim 10^{\beta_\gamma-1.9}\left(\frac{z+1}{3}\right)^{2\beta_\gamma+4}\frac{(\epsilon F_\epsilon)_{-9}}{\Gamma_{sc,3}^{2\beta_\gamma}\Gamma_{grb,2}^4t_{\gamma,1}^2}\ \frac{t}{1\rm ks}\,\epsilon_9^{2\beta_\gamma-1}\ . \quad (28)$$

In addition, the scattered photons can create pairs with GRB photons. The lab-frame energy of a GRB photon emitted at an angle $\theta>\Gamma_{grb}^{-1}$ relative to the radial direction of flow is a factor $(\Gamma_{grb}\theta)^2$ smaller than if the photon were released

at $\theta<\Gamma_{grb}^{-1}$. Then the condition for pair-formation leads to a minimum energy of the target photon (as measured by the observer if that photon were emitted at $\theta<\Gamma_{grb}^{-1}$) that is independent of θ:

$$\epsilon_t^{(grb)} = 0.60\,[(z+1)/3]^{-2}\Gamma_{grb,2}^{-2}\epsilon_9^{-1}\ \mathrm{MeV}\ . \quad (29)$$

Further, it can be shown that, owing to the scattering outflow being behind the GRB source, the scattered GeV photons can interact only with burst photons that have been emitted at an angle larger than $\theta_{min}(t_{lag}) = (ct_{lag}/R_\gamma)^{1/2}$, with ct_{lag} being the separation between the place of scattering and the GRB source and $R_\gamma = \Gamma_{grb}^2 ct$ the radius of the latter. For $\Gamma_{sc}>\Gamma_{grb}$, photons scattered by the fluid at ct_{lag} behind the GRB source arrive at observer at time $t = t_{lag}$, thus $\theta_{min}(t) \simeq (t/t_\gamma)^{1/2}\Gamma_{grb}^{-1} = 0.1\,(t_3/t_{\gamma,1})^{1/2}\Gamma_{grb,2}^{-1}$. Taking into account that the lab-frame distribution GRB photons with angle θ relative to the radial direction of motion is $dN_{grb}/d\Omega \propto [\Gamma_{grb}(1 - B\cos\theta)]^{-2}$ (with B the speed the GRB source), the photons emitted at $\theta>\theta_{min}$ are a fraction

$$f(t) = (\Gamma_{grb}\theta_{min})^{-2} = t_\gamma/t \quad (30)$$

of the number of GRB photons

$$N_{grb} = \frac{4\pi d_l^2(z)}{(z+1)^2} t_\gamma F_p = 10^{59.3}\left(\frac{z+1}{3}\right)^2 \phi_{-5}\epsilon_{p,5}^{-1}\ . \quad (31)$$

Thus, the number of GRB photons above the threshold energy $\epsilon_t^{(grb)}$ that can reach the test photon is $N(>\epsilon_t^{(grb)}) = f(\epsilon_t^{(grb)}/\epsilon_p)^{-\beta_\gamma} N_{grb}$. Then, for the scatterer radius given in equation (27), equations (20) and (29)–(31), lead to the following optical thickness to pair-formation on burst photons

$$\tau_{sc,grb} \lesssim 10^{1.5-0.8\beta_\gamma}\left(\frac{z+1}{3}\right)^{2\beta_\gamma+4}\frac{\phi_{-5}}{t_{\gamma,1}}\frac{\epsilon_{p,5}^{\beta_\gamma-1}}{\Gamma_{grb,2}^{2\beta_\gamma+4}}\left(\frac{t}{1\mathrm{ks}}\right)^{-1}\epsilon_{-9}^{\beta_\gamma}\ . \quad (32)$$

Equations (28) and (32) show that GeV afterglow photons may be lost to pair-formation on upscattered photons or on burst emission. The energy above which this processes reduces the high-energy flux is strongly dependent on the Lorentz factor of the GRB source and, for pair-creation on the scattered emission, also on the Lorentz factor of the scattering outflow.

The KN effect reduces the GeV flux at photon energies approaching $\epsilon_* = \Gamma_{sc}\gamma_e m_e c^2/(z+1) = 2[(z+1)/3]^{-1}(\Gamma_{sc}\gamma_e)_4\mathrm{GeV}$. The KN cutoff energy ϵ_* is above the peak energy $\epsilon_p^{(sc)}$ of the scattered GRB emission (equation 14) if the scattering parameter $\Gamma_{sc}\gamma_e$ is less than $\Gamma_{grb}^2(m_e c^2)[(z+1)\epsilon_p]^{-1} = 2\times10^4[(z+1)/3]^{-1}\Gamma_{grb,2}^2\epsilon_{p,5}^{-1}$, for which $\epsilon_p^{(sc)}<3\,[(z+1)/3]^{-2}\Gamma_{grb,2}^2\epsilon_{p,5}^{-1}$ GeV. The cut-off at ϵ_* is sharp only if the scattering electrons are cold ($\gamma_e = 1$); in this case, owing to that Γ_{sc} is most likely below 10^4, the KN effect truncates the scattered spectrum above its peak energy.

3 CONCLUSIONS

We have assessed the ability of four mechanisms related to GRBs and their afterglows to produce LAT-detectable GeV emission during the early afterglow phase ($t \sim 1$ ks). We note that the expected GeV fluxes were calculated from afterglow and GRB observables (X-ray plateau flux, duration, and spectral slope; burst fluence, duration, and spectral properties), keeping to a minimum the use of specific model parameters that are not well determined.

Except for the hardest or longest & brightest GRBs, the large-angle emission released during the burst and arriving later at observer should not be detectable to LAT. With the exception of the hardest X-ray afterglows, detectable GeV emission is not expected from the same emission process that yields the X-ray emission, particularly if the X-ray afterglow is synchrotron emission from the forward shock.

The other two mechanisms discussed rely on the upscattering (either in the forward-shock or an other part of the relativistic outflow) of lower energy photons into the GeV range and offer better prospects for detection with LAT.

The self-Compton scattering of forward-shock synchrotron photons is expected to be above LAT's 1 ks sensitivity for X-ray afterglows with plateaus brighter than the average. This mechanism can be identified based on that the spectral slope of the GeV emission should be the same as for the X-ray afterglow ($\beta_{GeV} = \beta_x$). In addition the decay rates of the fluxes at these two energies should satisfy $\alpha_{GeV} = \alpha_x + (\beta_x + 1)/2$ (equation 13). Pair-formation may reduce the self-Compton scattering flux at 1 GeV (equation 25) if the peak energy of the self-Compton emission spectrum is below 100 keV or of the X-ray plateau emission is hard and extends well above 100 keV (equation 26).

Bulk-scattering of the forward-shock emission by a delayed outflow can explain the X-ray plateaus observed in many Swift afterglows if the scattering outflow is pair-rich. The same mechanism may produce GeV emission that LAT can detect if the afterglow X-ray emission is brighter and harder than average. Scattering of the burst prompt emission may also produce detectable GeV emission, particularly for bursts brighter than average and afterglows with short-lived X-ray plateaus (equation 19). The upscattered emission should have the same spectral slope as the burst ($\beta_{GeV} = \beta_\gamma$) but can exhibit a variety of decays, depending on the radial distribution of mass and Lorentz factor in the scattering outflow. For this mechanism, pair-formation on either the burst photons or the upscattered emission itself reduces the GeV flux above a photon energy that is strongly dependent on the Lorentz factors of the GRB source and scattering outflow (equations 28 and 32). Consequently, the detection of photons above 1 GeV during the early afterglow can be used to set lower limits on these Lorentz factors, similar to how it was done for the GRB source Lorentz factor using the detection of 0.1–10 GeV photons during the burst by CGRO/EGRET (e.g. Fenimore, Epstein & Ho 1993, Baring & Harding 1997, Lithwick & Sari 2001).

For an effective area of 8000 cm^2, LAT's sensitivity corresponds to several GeV photons detected in 1 ks. Thus, for most GeV afterglows, the high-energy light-curve will be too crude for a determination of its power-law decay rate. As the spectral slope can be determined with a modest number of collected photons, comparing the slope of the GeV spectrum with those of the burst and X-ray afterglow emission provides a better way to identify the mechanism that produced the high-energy afterglow. For GRB 940217, the only burst for which GeV afterglow emission was detected so far, EGRET observations (Hurley et al 1994) show a hard component at 0.1–4 GeV, with $F_\epsilon \propto \epsilon^{1/3}$ during the burst and, possibly, during the afterglow, at 5 ks. The hardness of the

GeV emission suggests that it is the burst emission below its spectral peak upscattered by a lagged outflow.

We conclude by noting that, within the framework of the GeV afterglow emissions analyzed here, LAT will detect high energy photons under favourable conditions. GRBs dimmer or harder than the average and X-ray afterglows with dim and long plateaus could be accompanied by GeV emission that is too faint to be detected by LAT.

ACKNOWLEDGMENTS

The author acknowledges the support received from NASA Swift GI grant NNG06EN00I and LANL 20050161DR funding of Raptor

REFERENCES

Baring M., Harding A., 1997, ApJ, 491, 663
Burrows D. et al, 2007, Phil Trans A, 365, 1213
Chincarini G. et al, 2007, ApJ, submitted (astro-ph/0702371)
Dermer C., Chiang J., Mitman K., 2000, ApJ, 537, 785
Fan Y., Piran T., 2006, MNRAS, 370, L24
Fan Y., Piran T., Narayan R., Wei D., 2007, MNRAS, accepted (arXiv:0704.2063)
Fenimore E., Epstein R., Ho C., 1993, A&AS, 97, 59
Galli A., Piro L., 2007, A&A, accepted (arXiv:0705.4061)
Hurley K. et al, 1994, Nature, 372, 652
Kumar P., Panaitescu A., 2000, ApJ, 541, L51
Kumar P. et al, 2007, MNRAS, 376, L57
Liang E., Zhang B-B., Zhang B., 2007, ApJ, 670, 565
Lithwick Y., Sari R., 2001, ApJ, 555, 540
Lyutikov M., 2006a, New J. of Phys., 8, 119
Lyutikov M., 2006b, MNRAS, 369, L5
Mészáros P., Rees M., 1994, MNRAS, 269, L41
Mészáros P., Rees M., 1997, ApJ, 476, 232
Nousek J. et al, 2006, ApJ, 642, 389
Nugis T., Lamers H., 2000, A&A, 360, 227
O'Brien P. et al, 2006, ApJ, 647, 1213
Panaitescu A., Mészáros P., 1998, ApJ, 501, 772
Panaitescu A., 2005, MNRAS, 363, 1409
Panaitescu A. et al, 2006a, MNRAS, 366, 1357
Panaitescu A. et al, 2006b, MNRAS, 369, 2059
Panaitescu A., 2007, MNRAS, accepted (arXiv:0708.1509)
Pe'er A., Waxman E., 2005, ApJ, 633, 1018
Preece R. et al, 2000, ApJS, 126, 19
Rees M., Mészáros P., 1994, ApJ, 430, L93
Sakamoto T. et al, 2007, ApJS, accepted (arXiv:0707.4626)
Shen R., Barniol Duran, R., Kumar P., 2007, MNRAS, accepted (arXiv:0708.1649)
Wang X., Li Z., Mészáros P., 2006, ApJ, 641, L89
Watson D. et al, 2006, ApJ, 652, 1011
Willingale R. et al, 2007, ApJ, 662, 1093
Zhang B., Mészáros P., 2001, ApJ, 559, 110
Zhang B. et al, 2006, ApJ, 642, 354